Zygotic Expression of the *caudal* Homolog *pal-1* Is Required for Posterior Patterning in *Caenorhabditis elegans* Embryogenesis

Lois G. Edgar, Stephen Carr, Hong Wang, and William B. Wood

Department of Molecular, Cellular, and Developmental Biology, University of Colorado, Boulder, Colorado 80309-0347

Previous work has shown that the *Caenorhabditis elegans* gene *pal-1,* a homolog of *Drosophila caudal,* is required maternally for blastomere specification in the early embryo and postembryonically for tail development in males. We show here that embryonic (zygotic) transcription of *pal-1* is also required for posterior patterning during later embryogenesis. Embryos homozygous for strong loss-of-function mutations arrest as nonviable L1 larvae with gross posterior defects. PAL-1 protein produced from zygotic transcripts is expressed dynamically during gastrulation and morphogenesis in specific cells of all major lineages except the germ line. Most expressing cells are undergoing cell movements or forming midline structures or both. Mutant embryos exhibit defects involving most of the expressing cells. Aberrant early cell positions are observed in posterior hypodermis, both in the C-lineage cells that express *pal-1* and in the neighboring hypodermal seam cell precursors, which do not, as well as in posterior muscle derived from the C and D lineages. Defects in late gastrulation, ventral hypodermal enclosure, and formation of the rectum result from failures of cell movements of ABp and MS descendants. Limited mosaic analysis supports the view that most of the required *pal-1* functions are cell autonomous. © 2001 Academic Press

Key Words: cell movements; embryogenesis; embryonic lethals; gastrulation; morphogenesis; mosaic analysis; Nob mutants; patterning defects.

INTRODUCTION

Specification of early blastomere fates in *Caenorhabditis elegans* embryos involves segregation of cytoplasmic factors, differential translational controls, and inductive cell interactions during early cleavage stages (for reviews see Schnabel and Priess, 1997; Rose and Kemphues, 1998). Similar mechanisms are seen in the early development of echinoderm and amphibian embryos (reviewed in Davidson, 1991, 1994). In *Drosophila,* some steps in early patterning also involve localized translational repression of certain maternally supplied mRNAs, which may represent a common mechanism of establishing anterior–posterior (A/P) (or animal/vegetal) polarity in worms (Evans *et al.,* 1994), flies (Lehmann and Gavis, 1994), and frogs (Masquera *et al.,* 1993). In other respects, the early syncytial embryos of *Drosophila* are patterned by mechanisms not likely to operate in cellular embryos.

However, the later specification of regional identities along the A/P axis appears to include mechanisms that may be universal among metazoans. The Hox genes that specify segment identities in *Drosophila* have homologs that function similarly in all animals so far examined (reviewed by McGinnis and Krumlauf, 1992; Manak and Scott, 1994). Although *C. elegans* is not segmented, it exhibits metamerism in the form of repeating patterns of cell sublineages along the A/P axis which are modified differently in different body regions for generation of particular structures (Sulston and Horvitz, 1977; Sulston *et al.,* 1983). Some of these differences are controlled by Hox genes that appear homologous to those of *Drosophila* and vertebrates (Kenyon and Wang, 1991; Wang *et al.,* 1993; Clark *et al.,* 1993; Van Auken *et al.,* 2000).

Similar hierarchies of regulatory stages in patterning, including specification of axes and early cell fates, formation of metameric patterns, and eventual establishment of regional identities under control of Hox genes, may operate in most if not all embryos. However, current knowledge is still fragmentary regarding the events in cellular embryos that link early cell fate determination to later regional specification.

To gain further insight into these mechanisms, we undertook screens for non-maternal-effect mutants of *C. elegans* with embryonic patterning defects. In screening for potential patterning mutants, we have used primarily the mutagen trimethylpsoralen (TMP), which causes a relatively high frequency of small deletions (Yandell *et al.,* 1994), thus increasing the probability of strong loss-of-function mutations with accompanying DNA polymorphisms. Among the mutants obtained, we have identified mutations at five loci that result in embryos with fairly normal anterior development but severely defective posterior development (Nob phenotype). We report here on characterization of embryonic expression and function of a locus originally designated *nob-2,* which we have shown to be the same as the *C. elegans caudal* homolog *pal-1,* originally defined by a single mutant allele causing postembryonic defects in male tail development (Waring and Kenyon, 1990, 1991). Our identification of strong loss-of-function *pal-1* alleles led to the demonstration of a maternal requirement for *pal-1* function in specification of early embryonic blastomeres in the C and D lineages (Hunter and Kenyon, 1996). We show here that in addition, function of PAL-1 protein from embryonically produced (zygotic) transcripts is required for several aspects of posterior patterning during later embryogenesis. Zygotic *pal-1* function is required in the C and D lineages for axis establishment and patterning of the dorsal epidermis and posterior body musculature during gastrulation. It is also required in the AB and MS lineages for completion of gastrulation, ventral movement of lateral hypodermal cells to enclose the embryo during early morphogenesis (epiboly), and formation of the rectum. Mosaic analysis indicates that most of these functions are cell autonomous.

MATERIALS AND METHODS

Strains and Culture Methods

C. elegans strains were cultured and multiple mutants constructed by standard methods (Sulston and Hodgkin, 1988). Mutations and chromosomal rearrangements used were linkage group (LG) III, *dpy-17(e164); dpy-18(e364); unc-32(e189); unc-36(e251); unc-79(e1068); ncl-1(e1865); pal-1(e2091); sDp3 (III;f); qC1; rhDf1; sDf130; LGIV, him-8(e1489); LGV, him-5(e1467).* Most mutant strains were obtained from our collection or the *C. elegans* stock center (University of Minnesota), in addition to strains carrying *pal-1(e2091)* from C. Kenyon, *rhDf1; sDp3* from K. Nishiwaki, and *qC1* from J. Kimble.

Mutagenesis Screens

In general screens for LGIII embryonic lethal mutations, L4 hermaphrodite worms of genotypes *unc-32 dpy-18* or *dpy-18 unc-25* were mutagenized by soaking 15 min in a saturated solution of TMP (HRI Associates, Berkeley, or Sigma) in M9 buffer (Yandell *et al.,* 1994) and irradiating with $600-700$ μW/cm^2 of long-wave UV light from a Blak-Ray lamp Model UVL-21, maximum emission 360 nm, for 10 to 30 s. Mutagenized animals were mated to *unc32*

dpy18/qC1 or *dpy-18 unc-25/qC1* males, respectively. Wild-type cross progeny were cloned singly and scored for absence of Unc Dpy progeny and the presence of dead embryos or abnormal hatching larvae. The noncomplementing mutants *ct224* and *ct281* were outcrossed five times and rebalanced with *qC1* or the free duplication *sDp3* for phenotypic analysis.

Analysis of pal-1 Deletions

Genomic sequence of *pal-1* was obtained for both strands by standard methods using PCR primers designed from the cDNA sequence (Waring and Kenyon, 1991) and was subsequently confirmed by the *C. elegans* Sequencing Consortium (1998). The regions deleted by the mutations *ct224* and *ct281* were initially identified by Southern blotting, and breakpoints were then defined by sequencing PCR products amplified from homozygous mutant embryos using the primers DM-2 (5′TGTCGGTCGATGT-CAAGTCG) and DMR-6 (5′TGTGGAGTTAGAAACTACAGT) for *ct224* and DM-3 (5′TGATTTGGCACAGAGATGAA) and DMR-5 (5′AGAGTAAAGGATTGGAGACAGA) for *ct281.*

Analysis of pal-1 mRNAs

Worms of specific developmental stages as well as populations of mixed-stage embryos were prepared by collecting embryos after NaOCl treatment of gravid hermaphrodite worms, hatching the larvae in the absence of food to synchronize them, and feeding for appropriate periods before RNA isolation (Sulston and Hodgkin, 1988). Early embryo populations (<30 nuclei) were prepared by the method of Schauer and Wood (1990). RNA was isolated according to Perry *et al.* (1993). For RNA blot analysis, 10–12 μg of total RNA per lane was electrophoresed for 6 to 10 h at 50–75 V in 1.2% agarose gels containing 0.22 M HCHO in both gel and buffer. The RNA was transferred to a Zetabind membrane overnight and hybridized by standard methods with ^{32}P-labeled *pal-1* cDNA probe made by the random priming method or with digoxigenin-labeled RNA probes transcribed from the cDNA plasmid pPal-1 (gift from D. Waring and C. Kenyon). Filters were washed at 65°C in 1× SSC, 0.1% SDS for 4 × 30 min and exposed to Kodak X-ray film. Specific PCR-generated probes for exons 1, 3, 4, 5, and 6 were made by the random primer method using fluorescein-11–dUTP (Amersham) and detected with anti-fluorescein antibody and a chemiluminescence alkaline phosphatase reaction (Amersham); for exon 2, probe was transcribed using digoxigenin–dUTP (Boehringer Mannheim) and detected with antibodies to digoxigenin and a chemiluminescence alkaline phosphatase reaction.

The alternative 3′ ends of the cDNAs were cloned from PCR products amplified from a mixed-stage cDNA library (Okkema and Fire, 1994) using primers Ex5F to exon 5 (5′ATGTCCGTGTAC-GAACAGC) and λGT11F to the original λ phage vector (Gibco BRL; 5′ATTGGTGGCGACGACTCCTGGAG). The products were subcloned into the T7/T3 α18 vector (Gibco BRL) using *Hinc*II sites. From 10 individual subclones, PCR products were amplified using Ex6F, an exon 6 primer (5′GCGTGCAAAGGATCGTC-GTG), and λGT11F. Only two lengths, differing by approximately 200 bases, were found. When two (of eight) long and one (of two) short subclones were sequenced (DNA Sequencing Facility, Iowa State University), one of the long clones added poly(A) after nucleotide 1324, as does the Waring clone (Waring and Kenyon, 1991), the other after nucleotide 1316. The apparent poly(A)-addition signals are AATGAA (1307–1312) and AACAAA (1299–1304), respectively, both 12 nucleotides upstream. The short sub-

clone added poly(A) after nucleotide 1108, using the signal AATGAA (1089–1094), 14 nucleotides upstream. Although a fourth possible poly(A) addition signal, AACTAA, exists at nucleotides 1069–1074, we did not recover a cDNA of this length; no other signals are apparent between the two pairs of possible signals.

Transgenic Lines

To assay rescue of *pal-1* mutant strains, and for construction of lines expressing reporter gene constructs, worms were transformed by injection of cloned DNAs at 10–100 μg/ml according to published methods (Mello and Fire, 1995). pWPK6, pWK9, pWK14, and pPAL-1 cDNA were gifts from C. Kenyon and D. Waring (Waring and Kenyon, 1990, 1991). The plasmid pRF4, conferring a dominant Roller phenotype, was used at 100 μg/ml to identify lines transmitting an extrachromosomal array of the introduced DNAs. Vectors for construction of *lacZ* and GFP reporter constructs were pPD95.10 and pPD95.67, respectively (Fire *et al.,* 1990). *pal-1::lacZ* reporter constructs pSC3 and pSC22 were constructed using *Kpn*I/*Sal*I genomic restriction fragments containing 4.7 and 7 kb upstream of the *pal-1* initiation codon, respectively, and *pal-1* genomic sequence extending to the *Sal*I site in exon 5, inserted into pPD95.10. The *pal-1::gfp* reporter construct pRGHW1 contained the same *pal-1* sequence as pSC22, inserted into pPD95.67 (see Fig. 2). pSC16 replaced genomic with cDNA sequence in the genomic plasmid pWK14 (Waring and Kenyon, 1991) from the exon 5 *Sal*I site (5′) to the vector *Sal*I 3′ site (vector IBI130). To integrate extrachromosomal arrays into the genome, transgenic L4 animals were γ-irradiated with 3000 rads from a ^{137}Cs source, and their Roller progeny were screened for 100% transmission in the F2 generation. Integrated lines were outcrossed at least twice before analysis. The *myo3::gfp* plasmid pPD93.97 was obtained from A. Fire (A. Fire, S. Xu, J. Ahnn, G. Seydoux, pers. comm.). The transgenic reporter line for seam cells, *wIS1,* was kindly provided by J. Rothman (Gendreau *et al.,* 1994).

Antibody and X-Gal Staining

Worm embryos were stained with anti-PAL-1 antibody following the methods described by Hunter and Kenyon (1996), with the modification that embryos were in some cases initially treated with chitinase to remove the eggshell (Edgar, 1995). Staining was detected with Texas red-labeled goat anti-rabbit secondary antibody (The Jackson Laboratory). In some cases nuclei were stained with DAPI at 1 μg/ml in PBS.

For double staining of PAL-1 and LIN-26, embryos stained for PAL-1 as above were subsequently incubated with anti-LIN-26 antibody (gift from M. Labouesse; Labouesse *et al.,* 1996) and detected with FITC-labeled goat anti-rabbit secondary antibody (The Jackson Laboratory).

For staining of hypodermal cell boundaries, the monoclonal antibody MH27 (Francis and Waterston, 1985) was used, following the procedures detailed in Podbilewicz and White (1994). Staining was detected with a TR-labeled secondary antibody (DAM IgG; The Jackson Laboratory). Similar procedures were used to stain muscle using the monoclonal anti-myosin-heavy-chain antibody 5.6.1 (gift from D. Miller).

For double staining with MH27 and anti-β-Gal, methanol-fixed embryos were incubated with either a mouse monoclonal (Promega) or a rabbit polyclonal (5′ → 3′) anti-β-Gal antibody and detected with FITC or TR-labeled secondary antibodies (The Jackson Laboratory). Subsequently, slides were stained with MH27 as described above.

X-Gal staining followed methods previously described (Edgar, 1995). For postfixation detection of GFP reporters, embryos were fixed as for X-Gal staining and observed using Chroma Filter Set 41018 at 1000×.

Cell Lineaging

Four- to eight-cell mutant and wild-type embryos from *pal-1(ct224)/qC1* (BW1566) hermaphrodites were mounted on 5% Noble agar pads and recorded using a Leitz DMXE microscope equipped for multiple-focal-plane time-lapse video (4D) recording (referred to subsequently as the 4D-VRS) using originally the software designed by Fire (1994) and subsequently that of Thomas *et al.* (1996). Generally, sets of 25 optical sections (1.0 μm) were recorded at 20- or 30-s intervals for a period of 5 to 6.5 h. Images were compressed and transferred to optical or CD-ROM disks for analysis. Due to optical limitations, lineages could be analyzed to completion only in the top half of embryos mounted normally for lateral observation; consequently, embryos were mounted ventral- or dorsal-side up for following some lineages. For identification of PAL-1::GFP-expressing cells, the strain used was BW1851 [*pal-1::gfp* (*ctIS33*)], an integrated line carrying the constructs pRGHW1 and pRF4. A maximum of three time points with epifluorescence settings was recorded to avoid the slowed development or lethality that resulted from more exposure to the UV epi-illumination.

Mosaic Analysis

The strains used for mosaic analysis were *pal-1(ct224) dpy-17(e164) ncl-1(e1865) unc-36(e251)* III; *sDp3(III;f); him-8(e1489)* IV; and *pal-1(ct224) dpy-17(e164) ncl-1(e1865) unc-36(e251)* III; *sDp3 (III;f); him-8(e1489)* IV; *myo-3::gfp(ctIs34)* (unmapped, but not on LGIII). Mitotic loss of the free duplication *sDp3* occurs in approximately 1/200 cell divisions (Kenyon, 1986). Unc-36 animals (AB losses) and animals with less severe phenotypes than *ct224* homozygotes were scored for the cell-autonomous marker Ncl-1 (enlarged nucleoli) as L4 larvae or adults, using Nomarski optics at 1000×. The more severe phenotypes died as early larvae and were scored in defective L1 animals, which limited the cell types that could be reliably scored.

RESULTS

Analysis of nob Mutations at the pal-1 Locus

In screens for mutants exhibiting regional embryonic patterning defects, we observed a phenotype designated Nob (no back end), characterized by arrest at about the time of hatching with fairly normal pharyngeal and anterior development but a severely deformed posterior with a variable knob-like shape. A locus originally designated *nob-2* was defined by two noncomplementing mutations isolated following TMP mutagenesis, *ct224* and *ct281.* For both alleles, approximately 80% of homozygous mutant embryos (~20% of progeny embryos from a heterozygous hermaphrodite) arrest as Nob L1 larvae, most of which hatch and die within 48 h (Figs. 1B and 1C). Those remaining (~5% of progeny) do not hatch (Table 1), and Nomarski observation shows that they fail in posterior ventral hypo-
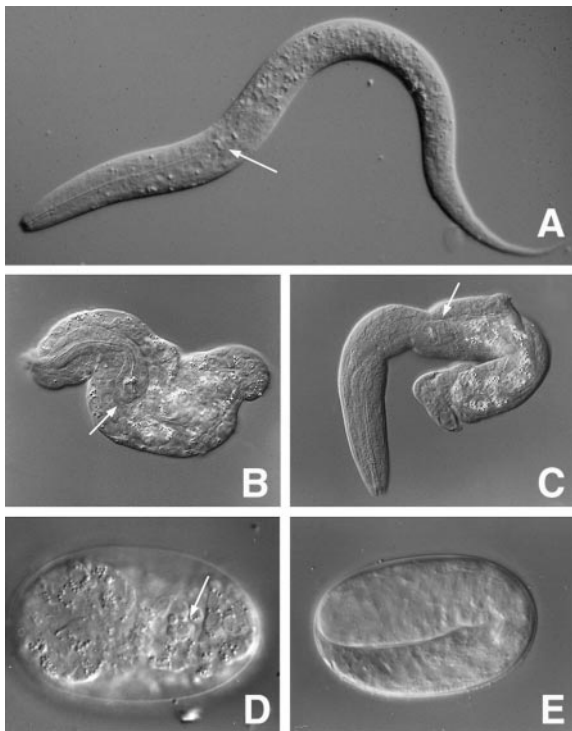
FIG. 1. Representative *pal-1(ct224)* mutant terminal phenotypes. *pal-1(ct281)* results in the same range of phenotypes. (A) Wild-type L1. (B, C) *ct224* short and long "Nobs." Arrows indicate the posterior end of the pharynx. (D) *ct224* unenclosed embryo; arrow indicates exposed gut cells. (E) Twofold wild-type embryo at same age as (D).

dermal enclosure (Fig. 1D). Genetic mapping by 2- and 3-factor crosses placed these mutations on linkage group III in the region of the *pal-1* gene. Both *ct224* and *ct281* failed to complement the previously described nonlethal *pal-1(e2091)* mutation (Table 2), which results in a postembryonic ray transformation in the male tail (Mab phenotype; Waring and Kenyon, 1990). This result suggested that *ct224* and *ct281* were either *pal-1* alleles or, since they were isolated following TMP mutagenesis, deletions that removed the *pal-1* locus as well as a nearby gene essential for viability.

Waring and Kenyon (1991) had cloned the *pal-1* gene and shown by cDNA sequencing that the predicted protein included a homeodomain similar to that of *Drosophila* Caudal. From genomic sequencing (subsequently confirmed and extended by the *C. elegans* Genome Sequencing Consortium) and comparison to the cDNA sequence, we determined the *pal-1* gene structure (Fig. 2). We also sequenced genomic fragments obtained by PCR from strains carrying *ct224* and *ct281* and showed that these mutations are small deletions of 4.2 and 4.7 kb, respectively, that remove part or most of the *pal-1* coding region (Fig. 2). To allow more rigorous phenotypic comparison with the nonlethal allele, we subjected *pal-1(e2091)* to several additional backcrosses,

which eliminated some of the originally reported embryonic lethality (Waring and Kenyon, 1991). In addition to viable adults with the Mab phenotype, the backcrossed strain produces about 0.5% arrested first-stage (L1) larvae with the Nob phenotype, and about half the viable L1 larvae exhibit a bulge near the middle of the animal that disappears in later larval stages (Table 2).

We carried out gene-dosage experiments using the small deficiency *rhDf1* (kindly provided by K. Nishiwaki), which deletes *pal-1* and the flanking genes *emb-5* and *dpy-17* (described in Ahnn and Fire, 1994). As shown in Table 2, both *ct224/rhDf1* and *ct281/rhDf1* genotypes cause Nob phenotypes similar to those of *ct224* and *ct281* homozygotes, respectively, suggesting that this phenotype results from strong loss of function at the *pal-1* locus. Unexpectedly, animals of genotype *e2091/rhDf1* have the same phenotype as *e2091* homozygotes, producing only a few percent Nob embryos and showing the L1 bulge and Mab phenotypes characteristic of *e2091* homozygotes (Table 2). By this genetic criterion *e2091* also behaves as a strong loss-of-function allele rather than a hypomorph, suggesting that it could result in loss of a separate, embryonically nonessential *pal-1* function in male tail development. Recent genomic sequencing in *e2091* has revealed an alteration in intron 5, which contains a control element for late embryonic *pal-1* expression in V6 (Zhang and Emmons, 2000).

On RNA blots, a *pal-1* probe recognizes two transcripts of 1.2 and 1.4 kb present at high levels in embryos and gravid adults and low levels during larval development and a transcript of approximately 3 kb present in L3 and L4 larvae, which we have not further investigated (Fig. 3A). The two smaller *pal-1* mRNAs are present at high levels in adult *fem-2(b245)* and *fer-1(hc1)* mutant animals, which contain oocytes but no fertilized embryos, but all mRNAs are absent in *glp-4(bn2)* mutant animals, which have no

TABLE 1

Phenotypes of Progeny Embryos from *pal-1(ct224)* Heterozygous Hermaphrodites

Parental genotype	Wild-type L1 (%)[a]	Nob (%)[b]	Unenclosed (%)[b,c]	Number scored
ct224/qC1				
Scored by Nomarski	72.0	21.5 (77)	6.5 (23)	339
Scored on plates	77.2	15.1 (66)	7.7 (34)	1283
ct224/ct224; sDp3				
Scored on plates	61.3	14.4	24.3	1660

[a] Genotypes *ct224/qC1* and *qC1/qC1* in approximate ratio of 2:1. The latter animals can be scored as sterile somewhat Dpy adults.
[b] Numbers in parentheses represent percentages of total homozygous *ct224* embryos.
[c] Scored on plates as unhatched embryos. This underestimates Nobs and overestimates unenclosed embryos, since a small percentage of Nob embryos do not hatch.

TABLE 2

Complementation and Gene Dosage Effects of *pal-1* Alleles

Genotype	Phenotypes
ct224/+	Wild type
ct224/ct224	~80% Nob, ~20% unenclosed
ct224/e2091	>99% viable Mab,[a] <1% Nob
rhDf1/+	Wild type (plus nonhatching embryos)[b]
rhDf1/rhDf1	Nonviable, nonhatching, unenclosed
ct224/rhDf1	Nob[b,c]
ct281/+	Wild type
ct281/ct281	74% Nob, 26% unhatched[d]
ct281/e2091	>99% viable Mab, <1% Nob[a]
ct281/rhDf1	Nob[b,c]
e2091/+	Wild type
e2091/e2091	~98% viable Mab, 0.5% Nob, 1.4% unhatched[e]
e2091/rhDf1	Viable Mab, 0.1% Nob[a,b,c,f]

[a] About half the viable L1's exhibit a midbody bulge that disappears in later larval stages.

[b] For all genotypes heterozygous for *rhDf1*, phenotypes listed are only those of hatching embryos, for the following reason. Self-progeny of *rhDf1/dpy-17 unc-36* hermaphrodites included 66% nonhatching eggs ($N = 1084$), whereas 25% would be expected if only *rhDf1/rhDf1* is lethal; among the viable offspring, the ratio of Dpy Unc to non-Dpy non-Unc progeny was 1:2, suggesting that the high proportion of nonviable progeny resulted from a maternal-effect haploinsufficiency that results in about a 50% survival rate for all genotypes except the *rhDf1* homozygotes. Consistent with this interpretation, progeny from two crosses of *him-5* males × *rhDf1/dpy-17 unc-36; fem-1(25°)* hermaphrodites (raised at 25°C to eliminate self-progeny) included 46 and 32% nonhatching eggs ($N = 419, 2867$).

[c] The genotypes *pal-1(ct224)/rhDf1, pal-1(ct224) dpy-17/rhDf1,* and *pal-1(ct281)/rhDf1* were produced by crossing *pal-1(ct224)dpy-17 unc-36, pal-1(ct224)dpy-17/dpy-17 unc-36,* or *pal-1(ct281)dpy-17 unc-36* males to *rhDf1/dpy-17 unc-36; fem-1* hermaphrodites raised at 25°C to eliminate self-progeny. The three crosses gave nonhatching embryos ranging from 26 to 66%; as in the control cross described in footnote (*b*), these were assumed to result from maternal haploinsufficiency affecting all progeny genotypes, plus an additional component of *pal-1/rhDf1* embryos corresponding to the 20% unenclosed (nonhatching) phenotype seen in *pal-1* embryos homozygous for *ct224* or *ct281* (Table 1). Taking these considerations into account, the Dpy, Dpy Unc, and Nob phenotypes among the hatching progeny of these crosses approximated the Mendelian ratios expected, with the hatching Nob phenotype ranging from 15 to 26%. ($N = 1924$ hatching animals from crosses with *ct224; N = 964* from the cross with *ct281*.) We therefore assumed that these Nobs represented the genotype *pal-1/rhDf1*.

[d] Scored on plates. See footnote (*c*), Table 1.

[e] Tested in a non-*him* background in a *pal-1(e2091) dpy-17* recombinant strain.

[f] Hatching progeny (55%) from the cross *pal-1(e2091) dpy-17/dpy-17 unc-36* males × *rhDf1/dpy-17 unc-36; fem-1(25°)* hermaphrodites were scored for the Nob phenotype (0.1% Nob, $N = 1326$). Male non-Dpy and non-Dpy non-Unc progeny ($N = 285$), representing the genotypes *pal-1(e2091)/rhDf1* and *e2091/dpy-17 unc-36* were scored for the *e2091* Mab phenotype; the 43% Mab males observed were assumed to represent the *pal-1(e2091)/rhDf1* genotype.

germ-line cells, showing that these transcripts are restricted to the germ line in adult hermaphrodites (Fig. 3B). At most stages, the 1.4-kb transcript is the most abundant. Probing of RNA blots with exon-specific probes and subsequent sequencing of the two cDNAs showed that all six exons are present in both, but that there is a difference in the 3′UTR sequences (see Materials and Methods).

Maternal and Zygotic Requirements for pal-1

By analyzing progeny from mosaic animals homozygous in the germ line for *ct224,* Hunter and Kenyon (1996) demonstrated that in addition to the zygotic requirement for *pal-1* function shown above, maternal *pal-1* function is also required in early embryogenesis, consistent with the abundance of *pal-1* message in the germ line (Fig. 3). In the wild-type embryo, PAL-1 protein is detected in the P_2 and EMS blastomeres of 4-cell-stage embryos. It is present in all the descendants of these cells until it begins to decrease at 24 cells, and by the 51-cell stage, it has disappeared from all but the P_2-derived C and D lineages (Hunter and Kenyon, 1996; Fig. 5A). To extend their analysis of early *pal-1* expression, we used a polyclonal antibody to PAL-1 protein (Hunter and Kenyon, 1996). In all embryos produced by *ct224/qC1* hermaphrodites, PAL-1 is detected from the 4-cell to the 28-cell stage, but in an increasing fraction of embryos it becomes undetectable after this point. By the 100-cell stage, 25% of the embryos exhibit no PAL-1 signal (Figs. 4A–4C). We assume that these represent the expected 25% of homozygous *ct224* embryos. This result indicates that all detectable maternally derived PAL-1 is lost by the 100-cell stage and that PAL-1 seen subsequently in the C and D lineages must be produced from zygotic transcripts.

To determine the extent to which the maternal and zygotic requirements are temporally and functionally distinct, we carried out transgene rescue and dosage experiments. Transgenic heterozygous *pal-1(ct224)/+* or *pal-1(ct281)/+* lines isolated after injection of genomic constructs carrying varying lengths of *pal-1* upstream sequence gave rise to viable *pal-1* homozygous mutant progeny which developed normally, indicating rescue as mentioned above. However, in most of the lines carrying these constructs either as extrachromosomal or as integrated arrays, the rescue persisted for only one generation; that is, homozygous mutant animals developed into adults that exhibited maternal-effect embryonic lethality, producing only nonviable Nob embryos. These embryos, unlike the Nob embryos from *pal-1* germ-line mosaic animals (Hunter and Kenyon, 1996), produced C and D lineage muscle. This limited rescue presumably results from insufficient transgene expression in the maternal germ line, which has been observed for most transgenes so far introduced into *C. elegans.*

Nevertheless, we did recover three lines (BW1598, BW1599, BW1600) that produced viable embryos and could be propagated as homozygous *pal-1(ct224)* strains. These carried integrated *pal-1*(+) transgenes derived from injec-
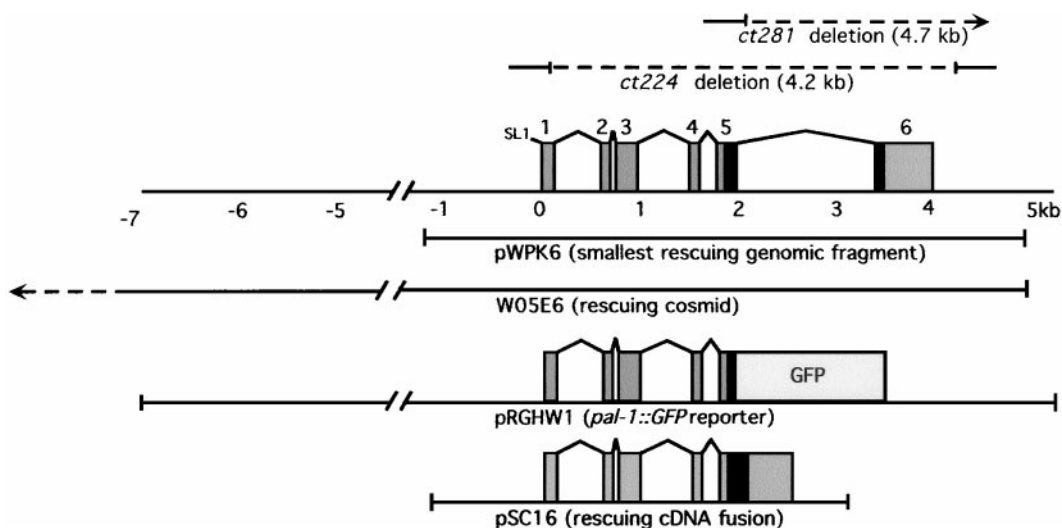
FIG. 2. Structures of the *pal-1* gene, mutants, and constructs. The *pal-1* gene structure is shown in the third line; the homeobox (exons 5 and 6) is indicated in black. Above, extents of the *ct224* and *ct281* deletions; below, constructs used in these experiments. The *lacZ* reporters pSC3 and pSC22 (not shown) were similar in structure to the GFP reporter pRGHW1, with 5 and 7 kb of upstream sequence, respectively. All three reporters showed essentially the same patterns of expression. Injection of the genomic–cDNA fusion construct pSC16 rescued either mutant, confirming that the *ct224* and *ct281* phenotypes result from loss of *pal-1* function.

tion of the entire cosmid WO5E6 (Fig. 2), which includes *pal-1* and at least 10 kb of upstream sequence. To ask whether this complete rescue resulted from maternal transcription or from embryonic transcription of the transgene, we examined early embryonic expression of the PAL-1 protein in several lines. In rescued *ct224/ct224* embryos from all lines tested with antibody staining, we detected no PAL-1 before the 28-cell stage, when it appears in the C and subsequently in the D lineage (Figs. 4D–4F). The relative embryonic viability of the three lines correlated with the intensities of antibody staining as embryonic PAL-1 expression became detectable. Therefore, the viable embryos produced in subsequent generations of strains BW1598, BW1599, and BW1600 are rescued either by a low but undetected level of maternal expression or by excess embryonic expression, resulting from the presumed higher than normal copy number of the *pal-1* transgenes.

Patterns of pal-1 Zygotic Expression

We analyzed zygotic expression of *pal-1* by antibody staining of wild-type animals, X-Gal staining of transgenic animals carrying *pal-1::lacZ* reporter constructs (primarily pSC3, with 5 kb, and pSC22, with 7 kb of upstream sequence), and lineage analysis of a strain carrying the integrated *pal-1::gfp* reporter transgene pRGHW1 (Fig. 2). PAL-1 produced from zygotic transcripts is seen initially in C and D lineage cells that also expressed maternally derived PAL-1. Representative expression at several stages is shown in Fig. 5, and the subsequent patterns of zygotic expression are summarized in Fig. 6. These patterns, described in detail
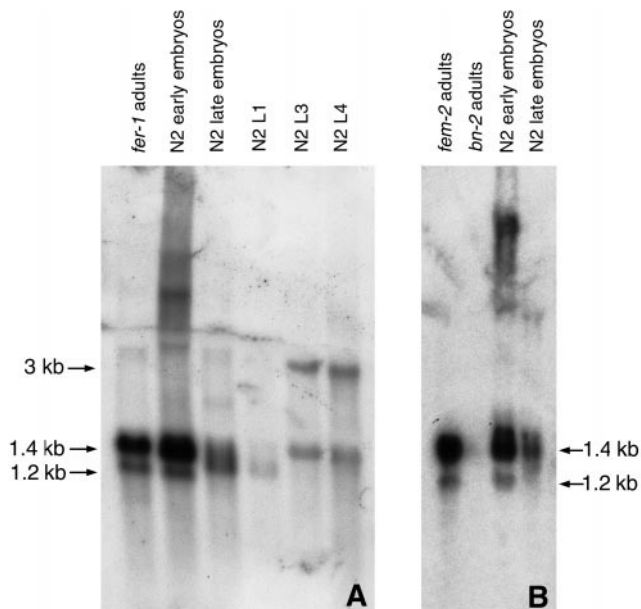

FIG. 3. Expression of *pal-1* during development and in the adult hermaphrodite germ line. (A) Hybridization of a *pal-1* cDNA probe to blots of RNA from embryonic, larval, and adult developmental stages. *fer-1* hermaphrodites produce no sperm and therefore contain no developing embryos. (B) A similar RNA blot demonstrating that adult *pal-1* expression is limited to the germ line. *fem-2* hermaphrodites have no sperm, hence no developing embryos; *glp-1(bn2)* hermaphrodites have no germ line.
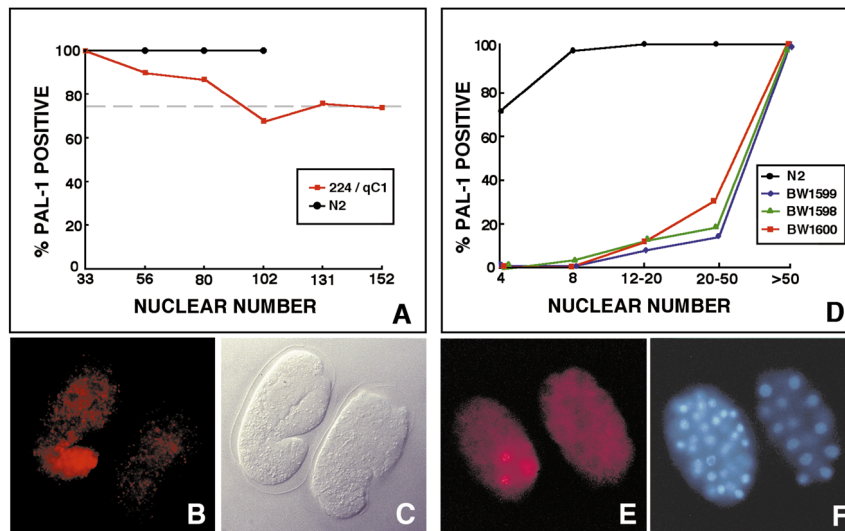
FIG. 4. The transition from maternal to zygotic *pal-1* expression. (A–C) Lack of zygotic expression in *pal-1* homozygous embryos. (A) % of PAL-1-positive embryos, determined by antibody staining, plotted versus embryonic age (nuclear number) in a population of self-progeny from hermaphrodites of genotype *ct224/qC1,* in which 25% of the embryos are *ct224/ct224* ($N > 44$ for each point; total $N = 573$). (B, C) Side-by-side comma-stage embryos (550 cells) of genotypes *ct224/qC1* (left) and *ct224/ct224* (right), stained with anti-PAL-1 antibody (B) and viewed with Nomarski optics (C). (D–F) Zygotic expression without maternal expression in homozygous *pal-1* embryos rescued by the injection of a wild-type *pal-1* gene. (D) % of PAL-1 positives plotted versus embryonic age for embryos from wild type and from BW1598, BW1599, and BW1600, three lines homozygous for *ct224* but rescued by injection and independent integration of the cosmid WO5E6, carrying the *pal-1* gene and >10 kb of upstream sequence ($N > 100$ embryos scored for each curve). Embryonic viability is 7% for strain BW1599 (in which 60% of the adult hermaphrodites are sterile), 91% for BW1598, and 95% for BW1600, which shows the strongest antibody staining. (E, F) Side-by-side 15-cell (right) and 51-cell embryos (left) of strain BW1599 stained with PAL-1 antibody (E) and DAPI for nuclear counts (F). The 15-cell embryo shows only background staining with antibody, i.e., maternally derived PAL-1 protein is undetectable (see Figs. 6A and 6B for comparison to wild type). In the older embryo, zygotically expressed PAL-1 is present in the four C cells.

in the legend to Fig. 5, can be summarized as follows. As gastrulation begins, expression is seen in only Ca and Cp (Hunter and Kenyon, 1996; Figs. 5A and 5B) and then in their daughters (Fig. 5C), of which 2 are hypodermoblasts (Caa and Cpa) and 2 are myoblasts (Cap and Cpp). The GFP reporter is first detected at the late 2C-cell stage and then more strongly in the 4 daughters (Fig. 5C). At about 100 cells, expression is also detected in the 2 D-lineage myoblasts. Thereafter, PAL-1 continues to be detected in all C and D descendants until the end of gastrulation at about 350 cells.

At about 180 cells (midgastrulation), the C hypodermal precursors, which express more strongly than the muscle precursors, form a characteristic double row on each side of the dorsal midline in the posterior (Figs. 5D and 5E). Thereafter, PAL-1 decreases in these cells and is no longer detectable with antibody after 350–500 cells. At about 250 cells, expression is detected in two AB cells that border the posterior left edge of the mesectodermal cell layer that is closing the ventral gastrulation cleft (ABplpapp and ABplppppp; Fig. 5F) and slightly later in the right homolog of one of them (ABprppppp). The daughters and granddaughters of these cells, generated after the cleft closes, continue to express strongly along

the ventral midline until about the time of hatching (Figs. 5G–5L). Beginning at about 360 cells, as morphogenesis begins, weak transient expression is detected in the posterior ectodermal P cells and occasionally in posterior V cells as both groups move ventrally (Figs. 5H and 5J). During this period the V cells become the lateral seam cells, and the P cells undergo their terminal embryonic divisions as they complete hypodermal enclosure of the embryo (Williams-Masson *et al.,* 1997).

Meanwhile, in the interior, *pal-1* expression, detectable both with antibody and with reporter constructs, appears at about 350 cells in 2 Ea descendents near the middle of the gut primordium (the int5 pair, Fig. 6L) and in 2 anteriorly located MS descendents which migrate to the posterior and become the mesoblast M and the right intestinal muscle (mu intR) (Figs. 5G and 5H). During early morphogenesis as the embryo develops through the comma stage (Figs. 5J–5L) and begins to elongate, all the *pal-1*-expressing cells (approximately 50) are located in the posterior ventral region, except for the 2 midgut cells which lie more dorsally. The descendants of ABpl/rppppp, as well as mu intR, move into the elongating tail and participate in formation of the rectal and associated intestinal muscles, as well as the ventral tail hypodermis.
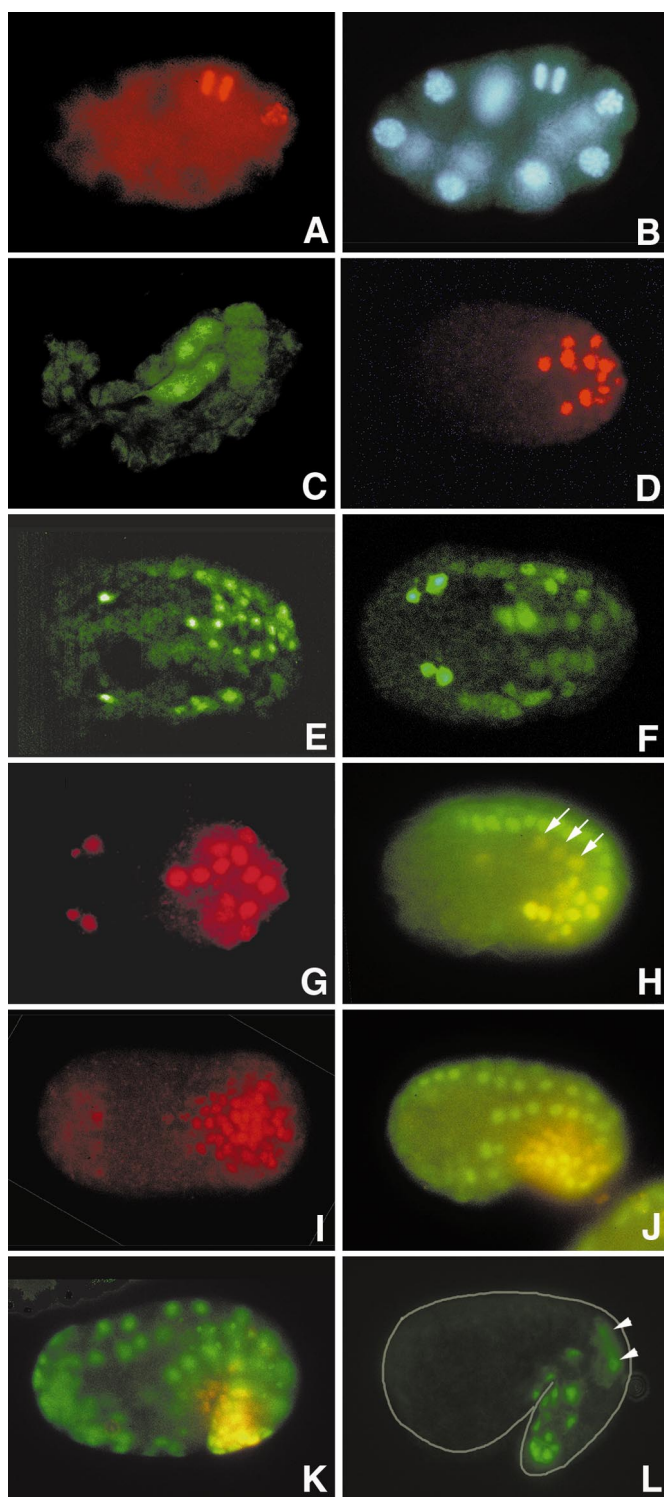
Expression diminishes during elongation and by hatching is detectable only in the 2 gut cells, M, mu intR, and 10 cells descended from ABpl/rppppp.

In summary, *pal-1* shows a dynamic pattern of zygotic expression in small subsets of cells from all lineages except the germ line. It also appears to be absent from all ABa-derived cells except for transient expression in the V6 cell at the start of morphogenesis (Hunter *et al.,* 1999). Most of the cells that express *pal-1* are moving or forming midline structures, or both, during the time of their expression.

FIG. 5. Expression patterns of *pal-1* during embryogenesis. Expression was visualized by staining with anti-PAL-1 antibody in wild-type embryos or with fluorescence in fixed embryos of the strain BW1851 carrying the transgenic *pal-1::gfp* fusion construct pRGHW1. Antibody staining generally matched the PAL-1::GFP fluorescence, but showed more positive cells during the lima bean stage, suggesting that not all upstream control elements may be present in pRGHW1 and less prolonged accumulation in C and D hypodermal and muscle cells, perhaps an effect of GFP perdurance. Nuclear numbers below 350 were counted in DAPI images (most not shown) of the corresponding embryos. All embryos are oriented with anterior to the left. (A, B) Maternal expression. Antibody staining (A) and DAPI (B) fluorescence images of a 15-cell embryo showing presence of PAL-1 protein in two C cells and P₃. *pal-1::gfp* is not expressed at this stage. (C) Onset of zygotic expression. The earliest expression of *pal-1::gfp* is in the four C cells of a 57-cell embryo. At this stage maternal translation product is disappearing. (D) Dorsal view of a 98-cell embryo. Both C-lineage hypodermal (double central row) and muscle (lateral cells) precursors stain with antibody. (E, F) Dorsal and ventral views of *pal-1::gfp* embryos at about 250 cells. C hypodermal (two middorsal rows) and C and D muscle progenitors (more lateral rows) are visible in the dorsal focal plane (E) and more faintly in the ventral view (F). C and D cells will shortly lose PAL-1 staining. The two MSxpaapp cells (E) and their four daughters (F) are visible in the anterior before the two MSxpaappp cells begin their posterior migration (and the two MSxpaappa cells undergo cell death). Ventrally, the two ABplpxppp cells are visible on the midline (F). (G) Ventral anti-PAL-1 staining at approximately 350 cells. The daughters of ABplpappp and ABplppppp, and also of ABprppppp, stain strongly, as well as some of the more lateral ABpxpppa descendants. (H) Lateral view at the same stage of an embryo stained with anti-PAL-1 (red) and anti-LIN-26 (green), which stains all hypodermal cells; costained cells are yellow. The lateral hypodermal cells P7/8, 9/10, and 11/12 (arrows) stain transiently during early morphogenesis. The single ABa-derived cell V6 also stains transiently at this stage (Hunter and Kenyon, 1999). (I, J) Ventral and lateral views at the lima bean stage, the onset of morphogenesis. Anti-PAL-1 staining (I) is maximal at this stage, in the daughters of the AB cells observed at the previous stage and additional ABpxpppp descendants, as well as the ABpxap descendants P7/8, P9/10, and P11/12. Not all cells have been identified, as staining is variable and transient, but the ABpxpppa-pap cells are likely candidates on the basis of both position and later staining. Costaining for LIN-26 (J) indicates that these are all hypodermal cells. (K) Early elongation. Most of the cells that earlier stained strongly continue to do so, but have moved into the tail. P7/8 and P9/10 can be detected only faintly with antibody. (L) 1½-fold embryo, PAL-1::GFP image. The AB cells forming tail and rectal structures continue to stain until hatching, and the two E descendants forming intestinal ring 5 are visible on the dorsal side (arrowheads). An outline of the embryo has been added for orientation.
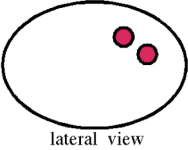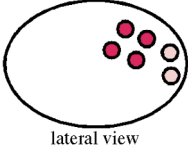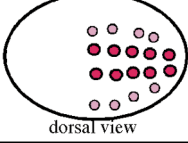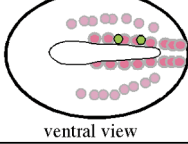
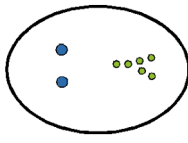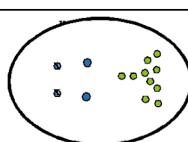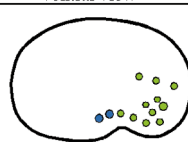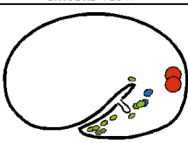| Age (min) Cell #	Pattern	Cell identification and cell fate
80 min 26 cells	lateral view	**2C: hypodermis, muscle**
140 min ~50 cells	lateral view	**4C: hypodermis, muscle** **2D: muscle**
195 min ~200 cells	dorsal view	**16 C** **8 D**
230-260 min ~250 cells	ventral view	**16 C** **16 D (faint)** **ABplpappp** **ABplppppp**
260-290 min ~300 cells	ventral view	**MSapaappp: mesoblast M, death** **MSppaappp: int mu R, death** **ABplpappa/p: rectal epithelium, neuron, K, K'** **ABplpppppa/p: anal depressor, int mu L, hyp 10, tail spike** **ABprpppppa/p: sphincter, body muscle, hyp 10, tail spike**
310-370 min 350-500 cells	ventral view	**MSapaappa/p** **MSppaappa/p** **ABplpappa/p** **ABplppppa/p** **ABprppppa/p** **ABplpppapap: hyp 8/9** **ABprpppapap: hyp 8/9**
lima 370 min 550 cells	lateral view	**MSapaappp** **MSppaappp** **ABpl/rappapp:P7/8** **ABplpppppaa/p ABpl/rapapap:P9/10** **ABplppppppa/p ABpl/rapappa:P11/12** **ABprpppppaa/p ABprpppapap:hyp 8/9** **ABprppppppa/p ABplpppapap:hyp 8/9**
1 1/2-fold 430 min 550 cells	lateral view	**MSapaappp** **ABprpppapap:hyp 8/9** **MSppaappp** **ABplpppapap:hyp 8/9** **ABplppppppaa/p** **ABplppppppa/p** **Ealpp:int ring 5** **ABprpppppaa/p** **Earpp:int ring 5** **ABprppppppa/p**

FIG. 6. Diagrams of *pal-1* embryonic expression patterns and identification of *pal-1*-expressing cells. Cells from various lineages are shown in different colors. The patterns shown are consensus patterns derived from staged embryos stained with PAL-1 antibody and from the line BW1851 carrying the integrated *pal-1::gfp* plasmid pRGHW1. Cell identifications are based on lineage data fom BW1851 embryos, antibody staining following laser ablation of suspected precursor cells, and double staining with PAL-1 antibody and tissue-specific antibodies.

Defects in Posterior Hypodermis and Muscle Resulting from Lack of Zygotic *pal-1* Expression

Defects in dorsal hypodermal development. In *ct224* homozygous embryos, we observed abnormal planes of division and cell contacts in the C lineage as early as the 28-cell (4C-cell) stage. The 28-cell embryo, just after gastrulation initiates, includes 16 cells of the AB lineage (ABxxxx), as well as the D founder cell, a myoblast, and 4 granddaughters of the C founder cell (Cxx), of which 2 are hypodermoblasts (Caa, Cpa) and 2 are myoblasts (Cap, Cpp; Sulston *et al.,* 1983). The 2 C cells of each fate eventually function as left–right (L/R) homologs, giving rise to equivalent and bilaterally symmetric sets of hypodermal and muscle cells on the left (Caa, Cap) and right (Cpa, Cpp), respectively, at the 350-cell stage. (Caa and Cpa produce hypodermal cells on the sides opposite to their origins because their immediate descendants intercalate and their nuclei change places during early morphogenesis, migrating across the dorsal midline to the opposite side of the dorsal hypodermis; Sulston *et al.,* 1983). However, at the 28-cell stage, as the result of the L/R asymmetry of early cleavages (Wood, 1998), all 4 C cells are asymmetrically positioned on the dorsal left side of the embryo (Figs. 6 and 7), produced by cleavages of Ca and Cp that are not strictly A/P but skewed roughly 30° from the embryonic A/P axis (Figs. 7A, 7B, and 7G). During early gastrulation, general bilateral symmetry of both the C hypodermoblast and the myoblast descendants is achieved by cell movements and progressive alignment of division orientations with the embryonic A/P axis.

Lineage analysis of three *ct224* embryos observed from the dorsal aspect showed that all C-cell divisions occurred at the normal times, with only one late exception (Table 3). However, variably abnormal cell positions and contacts in the quadrant of four C cells were seen in five of seven fully or partially lineaged mutant embryos (Figs. 7D, 7E, and 7G), while only one of seven *ct224/qC1* embryos showed a minor, transient abnormality in the position of the four C granddaughters. Subsequently in the mutant embryos, the double row of middorsal hyp7 precursor cells, normally oriented along the A/P axis (Fig. 7C), was skewed, and the right and left lineal homologs did not line up symmetrically along the dorsal midline. The contralateral nuclear migration that normally occurs in these cells at the onset of morphogenesis did not take place; the cells failed to elongate in either the circumferential or the A/P direction and instead formed isolated areas that appeared to differentiate as hypodermis (Fig. 7F) and later formed cuticle.

Abnormal behavior of nonexpressing hypodermal cells. Early abnormalities were also seen for AB-derived cells in which no *pal-1* expression was detected by either antibody staining or reporter expression. The more anterior region of the posterior dorsal hypodermis (hyp7 syncytium) forms from three AB hypodermoblasts, ABarpa, ABarpp, and ABplaa. By the end of gastrulation (~350 cells), their descendants are lined up symmetrically along the dorsal midline anterior to the C hypodermal cells. The AB- and C-derived
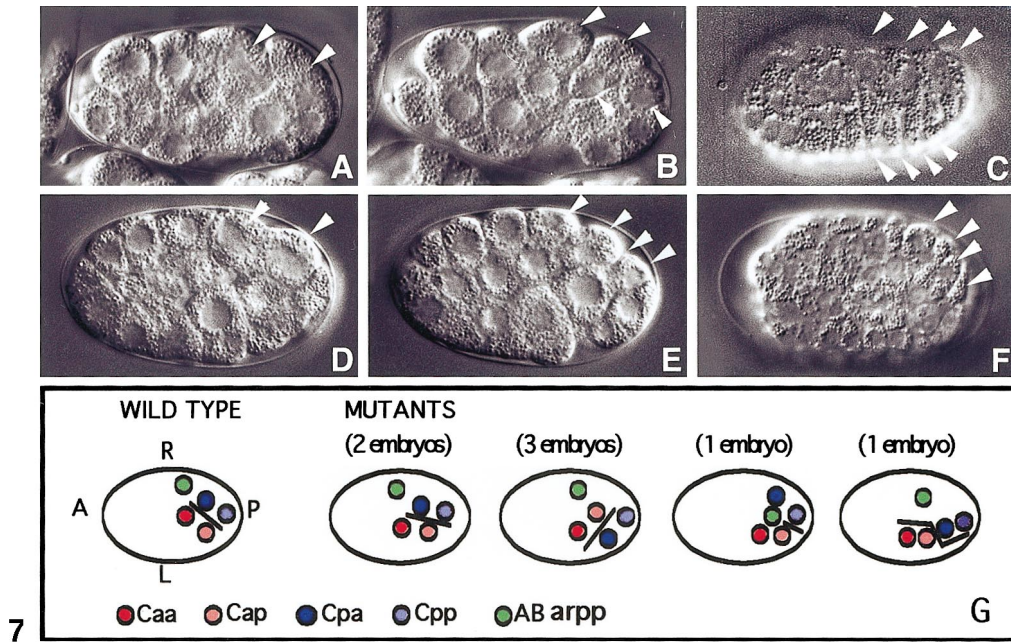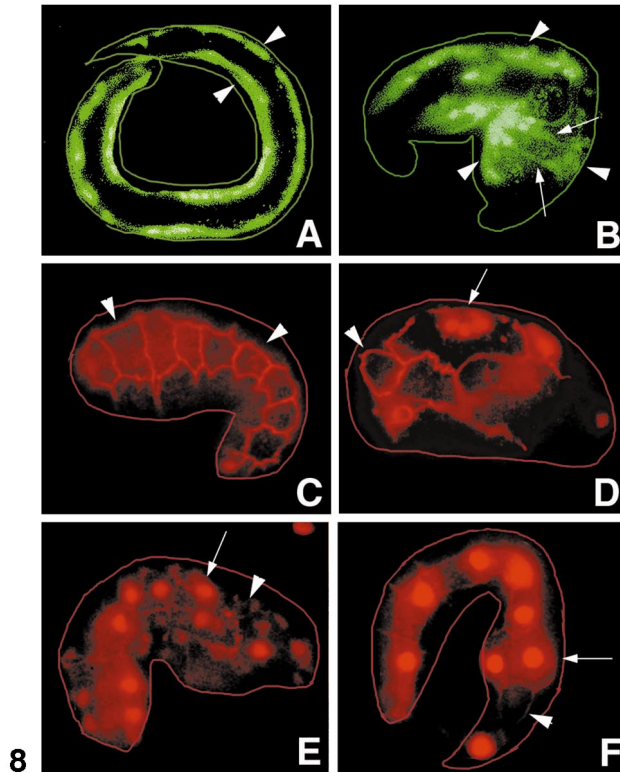
FIG. 7. Abnormal early C cell positions in wild-type and *pal-1* mutant embryos. Anterior is left, dorsal up. (A, B) Left lateral views of a wild-type embryo, genotype *ct224/qC1*, early and late in the 2C4 division (arrowheads indicate C cells). Note the oblique axes of division; the four C cells form a diamond pattern. Caa and Cpa are hypodermal precursors, and their descendants gradually assume an anterior–posterior alignment with further division, demarcating the middorsal plane. Caa descendants will stay on the left side and Cpa on the right until their nuclei migrate contralaterally at 310 min and the cells elongate laterally just before syncytial fusion of the dorsal hypodermis. Cap and Cpp are precursors of the posterior left and right body wall muscles, respectively (see text). (C) Dorsal view of C hypodermal cell arrangement in a wild-type embryo just before lima bean stage (about 350 min). The C cells (arrowheads) are elongating laterally and nuclear migration is in progress. (D, E) Left lateral view of the 2C4 division in a *pal-1(ct224)* mutant embryo. This division

TABLE 3

Lineage Abnormalities Observed in *pal-1* Mutant Embryos[a]

Lineage[b]	Tissue fate	Abnormalities observed
Ca, Cp*	Dorsal hypodermis, muscle	2C4 division at 28 cells. Cleavage axes abnormal, skewed; cell contacts of the four C cells abnormal (2/3 embryos).
Caa, Cpa, and descendants*	Dorsal hypodermis (hyp7)	Cells misplaced relative to their normal position flanking the dorsal midline; AB descendants sometimes intercalated; premature right/left fusions occur (3/3).
Cap, Cpp, and descendants*	Posterior muscle	Cleavage axes abnormal (2/3); right side muscles do not migrate as far as in wild type, and most posterior do not cross midline (1/3); final division may not always occur.
ABarpp and descendants	Dorsal syncytial hypodermis and seam hypodermal cells	ABarpp and descendants misplaced between Caa and Cpa from the 28-cell stage, forming only dorsal hypodermis (1/3). Some presumptive seam cells (by lineage) move into dorsal hyp7 positions rather than moving laterally (1/3).
ABarppxapa	Dorsal hypodermis (hyp7)	No contralateral migration (1/3); ABarpppapa acts like a V seam cell, moving laterally (1/3).
ABplpappp*, prpppppp*, and plpppppp*	Form borders of closing ventral cleft; contribute to rectal muscles and tail structures	Ventral cleft closure delayed (1/2, terminal phenotype Nob) or fails (1/2, terminal phenotype unenclosed). Cells divide prematurely, before meeting at the midline (2/2 embryos). Rectal and tail structures not formed (5/5).
MSapaapp* and ppaapp*	Mesoblast M and right intestinal muscle	Posterior migrations do not occur (2/2; additional embryos scored with *pal-1::gfp* reporter)
D and descendants*	Midbody muscle	No abnormalities observed (3/3).
E and descendants	Gut	No abnormalities observed; normal anterior–posterior orientation, in contrast to C cells (3/3).
P4 and descendants	Germ line	No abnormalities observed (2/2).

[a] Lineaging was performed by analyzing 6 to 7 h of development recorded with the 4D-VRS; three dorsally oriented mutants and two ventrally oriented mutants were recorded, as well as two wild-type embryos of the genotype *ct224/qC1*.

[b] Asterisk indicates that these cells would express *pal-1* in wild-type embryos at the time when abnormalities are observed in mutant embryos.

midline cells are flanked laterally by rows of 10 seam cell precursors on each side (H0, H1, V1–V6, and T), which are descendants of ABarpp (L/R: H2, V1, V2, V4, V6), ABplap (L: V3, V5, T), ABprap (R: V3, V5, T), ABplaa (L: H0, H1), and ABarpa (R: H0, H1). These cells are flanked in turn more ventrally by a row of P cells on each side, descended from ABplap and ABprap.

In the three dorsally lineaged *ct224* homozygous em-

is quite variable in mutants; in this case the axes are anterior–posterior and the four cells form a linear pattern. (F) C hypodermal cells in a terminal *ct224* mutant embryo (lateral view) well past the time of elongation, nuclear migration, and formation of the dorsal hypodermal syncytium in wild type. In the mutant the C cells are not elongated, nuclear movement is minimal, and syncytial fusion has not occurred. (G) Mutant variability at the 2C4 division in seven *ct224* embryos. Lines indicate the left–right (future midline) separation between Ca and Cp daughters.

FIG. 8. Aberrant posterior hypodermal and muscle patterning in *pal-1(ct224)* embryos. (A, B) Muscle; (C–F), hypodermis. Anterior is left, dorsal up in all images. Outlines of embryos were drawn from Nomarski images of the same preparations (not shown). (A) Wild-type late embryo expressing *myo-3::gfp,* a marker specific to body wall muscles. There are 81 body wall muscle cells arranged in four longitudinal quadrants, two of which are visible in this focal plane (arrowheads). (B) *pal-1(ct224); myo-3::gfp* terminal stage embryo, showing disruption of the muscle quadrant pattern, particularly evident as cell bridges (arrows) between quadrants (arrowheads). Muscle cell number is also reduced (see Table 5 and text). (C) Wild-type comma stage embryo, stained with MH27 antibody, a specific marker for gap desmosome junctions, which outlines hypodermal cell boundaries. At this stage, the dorsal and ventral syncytia have formed, and the lateral seam cells are outlined. Arrowheads indicate two seam cells. (D–F) Terminal stage embryos of the genotype *pal-1(ct224); wIS1* stained with MH27 and antibody to β-galactosidase, showing various frequently observed anomalies. *wIS1,* a *lacZ* reporter construct, is expressed in seam cell nuclei. (D) Embryo with extremely aberrant hypodermal cell boundaries and several seam cell nuclei within a syncytial cell boundary (arrow). Arrowhead indicates a presumptive seam cell with no *wIS1* expression. (E) Embryo showing lateral doubling up of V4 and V5 (arrow), with a gap at the V6 position (arrowhead). (F) Similar pattern in an L1 of the viable strain *pal-1(e2091); wIS1,* in which the larvae often have a ventral bulge near the midbody.

TABLE 4

Seam Cell and Body Wall Muscle Cell Numbers in *pal-1* Mutant Embryos[a]

Embryo genotype	Number of seam cells[b]		Number of muscle cells[c]		Phenotype
	Average	Range	Average	Range	
ct224/ct224;sDp3 or *ct224/qC1*	19.9 ± 2.1 ($N = 164$)	16–22	75.3 ± 4.4 ($N = 23$)	66–84	Wild-type
ct224/ct224	15.6 ± 3.2 ($N = 94$)	8–20	63.1 ± 7.2 ($N = 93$)	41–80	Nob

[a] Determined in separate experiments.

[b] Strains used carried an integrated *wIs1 lacZ* reporter construct specific for seam cells and were scored after X-Gal staining.

[c] Strains used carried an integrated *myo-3::gfp* reporter construct specific to body wall muscle and were scored by analysis of either confocal microscopic sections or optical sections recorded on the 4D-VRS.

bryos, the ABarpp-derived pair of dorsal hypodermal precursors just anterior to the C-derived hyp7 precursors also exhibited misalignment and no contralateral nuclear migration. Variable abnormalities were also seen in the ABarpp daughters, ABarppa and ABarppp (Table 3), which give rise, on the left and right sides, respectively, to H2 as well as V1, V2, V4, and V6. In the most extreme case, the descendants of ABarpppp assumed a position between the right and the left row of dorsal C hypodermal cells rather than lying laterally, and these descendants subsequently fused to the syncytium rather than differentiating as seam cells.

ABarpp descendants normally include both dorsal posterior hypodermis and seam cells; C hypodermal descendants produce only syncytial dorsal hypodermis. To test whether the above abnormalities reflected transformations of one hypodermal fate to another, we determined the number and position of seam cells in wild-type and *ct224* embryos at the stage when morphogenesis is normally complete. We identified seam cells using lines carrying *wIs1,* a *lacZ* reporter gene driven by a seam-cell-specific promoter (Hope, 1991; Gendreau *et al.,* 1994), and by staining with the antibodies MH27, which reacts with desmosomal junctions at the apical borders of all hypodermal cells (Priess and Hirsh, 1986; Waterston, 1988), and anti-β-galactosidase to identify the seam cell reporter. We found that *ct224* embryos have significantly fewer seam cells than normal embryos of genotype *ct224/ct224:sDp3* (Table 4), although lineaging had shown that these embryos made all the divisions needed to generate seam cells. In the mutant embryos, some laterally aligned cells in normal seam cell positions outlined by MH27 staining expressed neither *wIs1* nor *lin-26,* which is normally expressed in nuclei of all hypodermal cells including seam cells (Labouesse *et al.,* 1994) (Figs. 8D and 8E). A bunching up of the normally linearly arranged seam cells was frequently seen around the normal midbody position of V4 (Fig. 8E). Occasionally a syncytial fusion of cells expressing *wIs1* was observed (Fig. 8D). A similar overlap of seam cells near the V4 position was observed in late embryos produced by the viable mutant *pal-1(e2091),* which often hatch with a bulge near the middle of the larva (Fig. 8F). These observations indicate that *pal-1* mutations affect not only C-derived hypodermal

precursors, which express the gene, but also the posterior seam cell precursor ABarpp, which does not, suggesting that *pal-1* expression in the C lineage could generate secondary patterning signals required by neighboring AB cells.

Defects in posterior muscle development. We observed severe disruptions in the posterior muscle quadrants of Nob embryos, either by staining with the anti-myosin heavy chain monoclonal antibody 5.6.1 or by analysis of mutant embryos from the line BW1852 [*pal-1(ct224) dpy-17(e164) ncl-1(e1865) unc-36(e251); sDp3 III;f; ctIs34*], which carries an integrated *myo-3::gfp* construct expressed in body-wall muscle (Fig. 8B). In wild-type embryos, descendants of the two myoblasts Cap and Cpp form the posterior third of each of the four body wall muscle quadrants, and descendants of the D cell generate 20 more anterior body wall muscles. Because descendants of Cpp, which is located on the left at the 28-cell stage, must migrate around the developing gut to generate the right posterior body-wall muscles, some of the disruptions observed in the mutants probably result from failed movements of precursors in the early embryo. In two of three lineaged *ct224* Nob embryos, the four descendants of Cppp never moved as far anterior as normally. In one of these embryos, the most posterior, Cppppp, never crossed the midline, as defined by the normally oriented gut (Table 3). No highly abnormal final positioning was observed in D lineage muscle.

The final number of body wall muscle cells in mutant embryos was also reduced, from the normal 81 at hatching to an average of 63 (Table 4). This reduction could result from a failure of some C descendants to differentiate as muscle or from fewer than the normal number of C descendants. To distinguish these possibilities, we followed four embryos until the time of terminal division in the C lineage. In two dorsally lineaged *ct224* embryos, all C-lineage divisions up to the terminal one occurred normally. The final division, which normally separates the upper and lower muscle quadrants on each side of the embryo, was late, was D/V oriented, and could not be followed clearly from the dorsal aspect. In two ventrally lineaged *ct224* embryos, some of the C myoblasts were observed to undergo terminal divisions. However, others did not divide and instead showed characteristics of termi-

nally differentiated muscle cells before their normal time of division. Therefore, the observed abnormal muscle patterning in *ct224* embryos can probably be accounted for by a combination of early mispatterning and failure of some terminal divisions.

Defects in Later ABp and MS Lineages Resulting from Lack of pal-1 Expression

Defects in late gastrulation. Defects in late gastrulation were seen in two lineaged *ct224* embryos recorded from the ventral aspect, one of which terminated as a Nob, the other unenclosed (Table 3). In the wild-type embryo, completion of gastrulation occurs just before morphogenesis begins, at about 250 cells. Two pairs of mesectodermal left/right lineal homologs (ABpl/rpappp and ABpl/rppppp) move ventrally from their dorsolateral positions, forming the edges of a ventral cleft (Sulston, 1983; George *et al.,* 1997). The cells of the posterior pair (ABpl/rppppp) meet at the ventral midline, divide, and contact the most posterior of the C hypodermal cells (Caapv and Cpapv). These cells appear to adhere on contact, and the ventral cleft then zips up rapidly from posterior to anterior (see Figs. 9A–9C), allowing subsequent enclosure of the embryo by ventral movement of the hypodermis (epiboly). As noted above, the two left mesectodermal homologs (ABplpappp and ABplppppp) express *pal-1* during this closure and one of the right homologs (ABprppppp) shortly after the midline contact (Figs. 9D–9F).

In the Nob embryo (Figs. 9G–9I), the ventral cleft closed late and the bordering cells (ABpl/rpappp and ABpl/rppppp) divided prematurely, before they met at the midline. The ABpl/rppppp contacts with the posterior C hypodermal cells occurred but appeared to be transient. Subsequently, the P cells failed to migrate ventrally and hypodermal enclosure was delayed for at least 2 h. Although the hypodermis had enclosed the embryo after 12 h, no posterior elongation had occurred.

In the unenclosed *ct224* embryo the defects in cell movement during late gastrulation were much more severe (Figs. 9J–9L). The mesectodermal AB descendants that normally close the ventral cleft remained lateral, neither reaching the ventral midline nor contacting the posterior C hypodermal cells, and the ventral cleft failed to close. Subsequently, ventral hypodermal enclosure also failed, leaving the posterior gut and germ cells exposed on the ventral surface of the embryo.

Defective MS migrations. Defects in *ct224* Nob embryos were also observed in the two *pal-1*-expressing MS-derived mesodermal cells described above, mu intR and M. At the start of morphogenesis, MSapaap and MSppaap lie on the right and left of the pharyngeal primordium and divide to generate mu intR and M, respectively, as well as two anterior sister cells, which undergo programmed cell death. During morphogenesis mu intR and M are among the few embryonic cells which undergo a long-range migration, moving posteriorly along the ventral midline and reaching

their final posterior positions at about the lima bean stage. In a lineaged mutant embryo, as well as in observations of 12 mutant embryos carrying the *pal-1::gfp* reporter construct, these migrations never initiated, and the two cells remained near the pharynx at the normal time of hatching.

Defects in rectal and tail spike development. The *pal-1*-expressing cells ABplpappp, ABpl/rppppp, and MSppaapp normally generate one cell of the rectal epithelium, the anal depressor muscle, the two intestinal muscles, and the sphincter muscle, all rectal-associated structures. The ABpl/rppppp cell pair also generates the tail spike by posterior extension of the tail hypodermis (hyp 10). *pal-1Z*(−) Nob embryos do not show any identifiable rectal structures. The rectum is also lacking in wild-type embryos following laser ablation of the *pal-1*-expressing cell ABplppppp (L.E., unpublished results). The Nob embryos also lack a tail spike and show minimal posterior extension.

Mosaic Analysis of pal-1 Defects

To identify cells in which *pal-1* function is required, we performed a limited mosaic analysis, using two different strains. CF353 carried mutant markers in *dpy-17, unc-36, ncl-1,* and *pal-1(ct224)* on LGIII, complemented by wild-type copies on the free duplication *sDp3*. BW1852 had the same genotype except that it also carried an unlinked *myo-3::gfp* integrated transgene that could be used to identify body-wall muscle cells for reference. *sDp3* is lost somatically at a frequency of approximately 1 in 200 mitotic divisions (Herman, 1987). To identify mosaics, we scored initially for Dpy, Unc, or partial posterior (Nob-like) phenotypes and then determined the point of somatic duplication loss in the cell lineage by scoring the cell-autonomous Ncl-1 marker phenotype (enlarged nucleolus). Because Nob embryos are disorganized and arrest at L1 when the Ncl phenotype is difficult to recognize in many lineages, we scored primarily hatching animals with less severe phenotypes.

In control *pal-1*(+) strains, losses of the duplication at the first division in P_1 or in AB produce Dpy non-Unc and Unc non-Dpy phenotypes, respectively (Kenyon, 1986, and our unpublished experiments). In screening ~20,000 larvae from the *pal-1(ct224)* duplication strain, we recovered no Dpy non-Unc animals and 16 Unc non-Dpy animals, of which 15 could be attributed to meiotic recombination with the balancer duplication (Ncl in all nuclei). The remaining Unc was a mosaic with a loss in ABpla or ABpra. The absence of larvae with P_1 or AB losses can be interpreted to mean that lack of *pal-1* function in all the cells from either half of the lineage results in lethality. Consistent with this view, we found partial phenotypes resulting from later losses in both the P_1 lineage and the AB lineage. However, no losses in ABpl/rp were recovered among the less severe phenotypes, consistent with the involvement of these lineages in ventral cleft closure (but see Discussion).
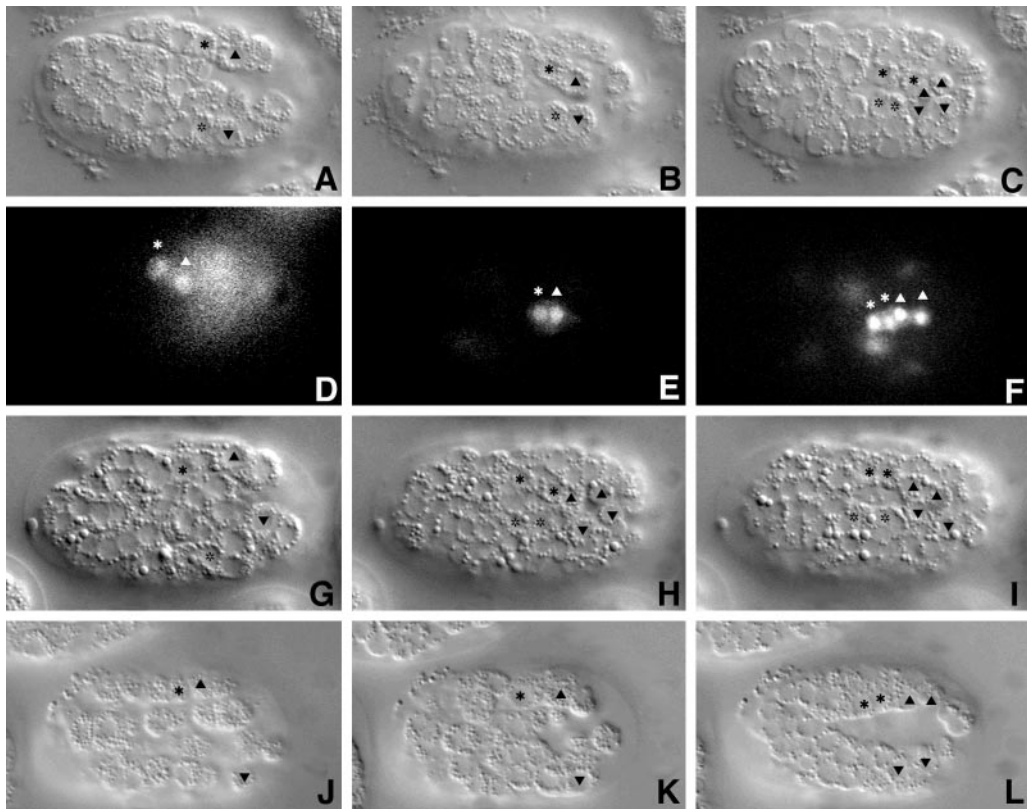
FIG. 9. Late gastrulation and ventral cleft closure in wild-type and *pal-1* embryos, imaged with the 4D recording microscope. All images are ventral views, and all are Nomarski images except for the epifluorescence images in D–F. Solid stars, ABplpappp; open stars, ABprpappp and their respective daughters; upward triangles, ABplppppp; downward triangles, ABprppppp and their daughters. (A–C) *ct224/qC1* normal embryo; (D–F) *pal-1*(+) embryo carrying *pal-1::gfp* (pRGHW1), showing reporter fluorescence; (G–I) *ct224/ct224* Nob embryo; (J–L) *ct224/ct224* unenclosed embryo. (A) 208 min after first cleavage: ridges of left and right AB lineage homologs move ventrolaterally to form the ventral cleft borders. (B) 244 min: ABplppppp and ABprppppp are the first cells to meet at the ventral midline and also contact Caappd/v and Cpappd/v just dividing at the posterior. (C) 252 min: the posterior ABs have divided, narrowing the cleft, and the anterior L/R pair (ABpxpappa) will divide shortly, to complete closure. (D) *pal-1::GFP* fluorescence of ABplpappp and ABplppppp in a wild-type embryo at 216 min. The diffuse fluorescence is from the C lineage hypodermal and muscle progenitors on the dorsal side of the embryo. (E) 262 min: the ventral cleft has just closed (compare with B). (F) 303 min: the ventral cleft has closed and ABplpappp and ABplppppp have divided. (G) *ct224* embryo (Nob terminal phenotype) at 195 min: the ventral cleft is forming, at a stage comparable to that of the wild-type embryo in (A). (H) 226 min: the ABpxpappp and AB pxppppp divisions are premature, occurring before the cleft closes. (I) 242 min: although the cleft is almost closed, as in wild type at this stage (C), it remained open in the middle until well after wild-type closure. (J) *ct224* embryo (unenclosed terminal phenotype) at 216 min: the lateral ridges have formed, as in wild type. (K) 254 min: the lateral ridges have moved very little and have not contacted the C posterior hypodermals. (L) 309 min: although the ABplpxppp and C divisions have occurred, the cleft remains open and it did not close through terminal arrest.

The losses resulting in posterior phenotypes that we were able to score are summarized in Table 5. Three embryos that appeared to have lost the duplication in either P_2 or C [so that the entire C lineage was *pal-1*(−)] displayed the Nob phenotype. Later losses in the C lineage or the D lineage resulted in elongated Nobs (Long Nobs) or regionally lumpy larvae, in which abnormalities appeared to correspond with tissues mutant for *ct224*. Severity of the defects, though somewhat variable, correlated approximately with how early the loss occurred.

DISCUSSION

Both Maternal and Zygotic pal-1 Expression Are Required for Embryogenesis

Our results demonstrate that in *C. elegans,* as in *Drosophila, Xenopus,* and mouse, the zygotic function of a *caudal* homolog is required for posterior patterning of the embryo. Both *pal-1* in *C. elegans* and *caudal* (*cad*) in *Drosophila* are transcribed maternally as well as in the

TABLE 5

Mosaic Analysis of *pal-1* Requirements

Phenotype	Observed losses[a]	Mosaics recovered
Nob	P$_2$ or C	3
Long Nob[b]	Ca or Cp (hypodermis and muscle)	2
	Cap or Cpp (muscle)	2
Lumpy[c]	Ca	1
	Cp	6
	Caa or Cpa (hypodermis)	5[d]
	Cap or Cpp (muscle)	13[d]
	D (muscle)	3
	ABarppxx (seam)	3
	ABplapapx (seam)	2
Unc non-Dpy	ABpla or ABpra	1

[a] Unenclosed phenotypes could not be reliably scored either for cell identification or for the *ncl-1* marker, and only a few of the least severe Nobs were scorable. However, no Dpy-17 animals (which would indicate a P$_1$ loss) were recovered; 15 or 16 Unc non-Dpy animals (which would indicate an early AB loss) were Ncl in all scorable nuclei and considered to arise from recombination with the balancer *sDp3*. Therefore, losses in either AB or P$_1$ are presumed to fall into the class of the most severe phenotypes. Note also that no ABpxpp losses were recovered.

[b] See text.

[c] Lumpy phenotypes were animals with localized defects, categorized as middle bulges, dorsal humps, tail lumps, and a missing or poorly developed rectum. Severe Lumpies do not survive to adulthood.

[d] Caa 2, Cpa 3 (these cells are L/R homologs); Cap 8, Cpp 5 (L/R homologs).

embryo. However, whereas either transcription mode alone is sufficient for normal embryonic development in *Drosophila* (Macdonald and Struhl, 1986; Mlodzik and Gehring, 1987), both modes of expression appear to be required in *C. elegans,* based on the findings of Hunter and Kenyon (1996) and our results.

Temporally, maternally and zygotically derived PAL-1 proteins overlap only slightly in their expression. In homozygous mutant *pal-1(−)* embryos produced by a *pal-1/+* hermaphrodite [*pal-1Z(−)* embryos], the maternally encoded PAL-1 protein, confined to the C and D blastomeres, fades rapidly after the 28-cell stage as also observed by Hunter and Kenyon (1996). Embryonic PAL-1 first appears in all 4 C granddaughters between the 28- and the 51-cell stage and in Da and Dp shortly after their birth in the same time interval.

The functions of maternally and zygotically expressed *pal-1* seem to be distinct. Maternal expression of *pal-1* is required specifically for determination of C- and D-lineage blastomeres as myoblasts. Although maternally supplied *pal-1* mRNA is present in all blastomeres at the four-cell stage, the activity of the PAL-1 protein is subsequently confined to C and D cells as the result of four controls: translational repression of *pal-1* mRNA by the *mex-3* gene

product as well as mRNA degradation in the AB cells, inhibition of function in EMS by SKN-1, and inhibition of function in germ-line cells by PIE-1 (Hunter and Kenyon, 1996). In the absence of maternal *pal-1* expression [*pal-1M(−)* embryos], the C lineage myoblasts Cap and Cpp, as well as the D myoblast, fail to produce muscle cells. This defect normally cannot be remedied by zygotic [*pal-1Z(+)*] expression. Conversely, C blastomeres from *pal-1Z(−)* embryos do produce muscle (Hunter and Kenyon, 1996). As we have shown, zygotic *pal-1* expression in the C and D lineages is required for other essential patterning functions, among which maintenance of myogenic capability is only a minor one as discussed further below.

Zygotic pal-1 Expression and Its Functions

The patterns of zygotic *pal-1* expression can be summarized and correlated with major events in late embryogenesis as follows (see Fig. 5). There is expression in the C and D lineages during early gastrulation. At this time, C-, D-, and AB-derived cells are moving to become symmetrically arranged around the dorsal midline, in preparation for later formation of the posterior muscle quadrants and dorsal hypodermis, as well as for lateral migration of the AB-derived V cells (seam cell precursors) and P cells to form the lateral and ventral hypodermis and the ventral nerve cord. Expression in other lineages is not seen until late gastrulation, when PAL-1 is detected in AB cells that form the edges of the ventral cleft prior to its closure and subsequently in ventrally migrating AB-derived seam-cell (V) and hypodermal (P) precursors that form the lateral and ventral hypodermis. Concurrently, it is seen in two MS-derived cells, which later migrate toward the posterior, and in two of the E-derived gut cells. The latter two cells are the two most posterior Ea descendants, which are unusual in that during gut formation they intercalate posterior to the most anterior Ep descendants and interact with the neighboring germ-line precursors Z2 and Z3.

It appears that *pal-1* function is required in most of these cells for the events in which they take part. We observed no obvious gut defects in these mutant embryos, suggesting that *pal-1* expression in the E lineage may be of only minor importance for gut formation. Otherwise, however, *pal-1Z(−)* embryos exhibit disorganization of C- and D-lineage cells during early gastrulation, as well as later failures in (1) nuclear migration in C-derived dorsal hypodermis, (2) separation of the C-derived posterior muscle quadrants, (3) ventral cleft closure, (4) ventral enclosure of the embryo by hypodermis, and (5) posterior migration of the MS-derived M mesoblast and mu intR cells.

Our mosaic analysis, although limited, supports the view that most of these functions are cell autonomous. For one of them, however, *pal-1* may act nonautonomously. Although no PAL-1 expression was detected in early seam cell precursors, *pal-1Z(−)* embryos show a significant reduction in seam cell number. Moreover, during formation of the dorsal hypodermis, not only C, but also AB precursors are mis-

aligned, although the AB cells do not express detectable PAL-1 during the period when misalignments were observed. Laser ablation experiments (L.E., unpublished results) strongly suggest that killing of C-lineage cells during early gastrulation affects positioning and subsequent contralateral nuclear migration in dorsal AB-lineage hypodermoblasts such as the major seam cell precursor ABarpp, in which no PAL-1 protein was detected. These results suggest that either (1) PAL-1 expression is required in these cells but at a level undetected by the antibody or (2) a secondary signal from *pal-1*-expressing C-lineage cells is required at the time of gastrulation for normal behavior of these AB-lineage cells. These alternatives were not distinguished by our mosaic analysis, because embryos that lost the duplication in the major seam-cell precursor ABarpp or its progenitors were not recovered among the viable mosaics analyzed. Failure to find these losses could have been by chance or because such embryos fail to enclose and hence were not scored. However, in a recent analysis of *pal-1(ct224)* mosaics for a different purpose, Hunter *et al.* (1999) reported two viable animals developing from embryos that had lost the *pal-1*(+) gene, one in ABar and one in ABpr, demonstrating that *pal-1* function is not required in any of the seam cell lineages for embryonic viability. This result, consistent with our expression and preliminary cell ablation data, strongly suggests that a secondary signal from the *pal-1*-expressing C-lineage cells at the early gastrulation stage is required for the normal positioning and later differentiation of the AB-derived seam cell precursors. This result also demonstrates that embryonic survival is not dependent on *pal-1* expression in ABprppppp and its descendants, which commences shortly after contact of this cell with its already expressing left lineal homolog at the midline in ventral closure (Figs. 9D–9F).

Targets of pal-1 Regulation

Although PAL-1 seems likely to have several regulatory targets, there is evidence at present for only two. One is the Hox gene *mab-5,* which is activated in the ABa-derived V6 cells during midembryogenesis. This activation requires *pal-1* function (Waring and Kenyon, 1990; Austin and Kenyon, 1994; Salser and Kenyon, 1996), and recent evidence indicates that *pal-1* may directly activate *mab-5* transcription in the V6 cells (Hunter *et al.,* 1999). *mab-5* could also require *pal-1* function for activation in the sex myoblasts descended from the M cell (Hunter *et al.,* 1999). Regulation by *pal-1* of another Hox gene, the posterior-group gene *egl-5,* would be consistent with the expression patterns of *pal-1* and *egl-5* in the late embryo (Cowing and Kenyon, 1992; Ferreira *et al.,* 1999), but at present there is no direct evidence for such regulation.

Another target for which there is evidence is *vab-7,* a homolog of the *Drosophila* pair-rule gene *even-skipped* (*eve*). Lack of zygotic *vab-7* function causes embryonic defects in embryonic C-lineage hypodermal and muscle patterning, but the embryos are viable. *vab-7* is expressed in

descendants of the four Cpxx cells, which generate the posterior set of right and left C-derived hypodermal and muscle cells (Ahringer, 1996). This expression has been shown to require maternal but not zygotic *pal-1* expression (Ahringer, 1997). However, the capacity to respond to ectopically expressed *pal-1* extends until morphogenesis (Ahringer, 1997), and in our cosmid-rescued lines, in which maternal *pal-1* expression was not detected, zygotically expressed *pal-1* may activate *vab-7.* Moreover, *pal-1* mutations and *vab-7* mutations cause very similar C-lineage phenotypes, suggesting that *pal-1* may function to maintain *vab-7* expression in the late embryo.

It is not clear whether any of these regulations is direct, but precedent from other organisms suggests that they could be. In mouse, in which lack of the *caudal* homolog Cdx-1 causes posterior-to-anterior vertebral transformations reminiscent of Hox gene defects, the Cdx-1 protein has been shown to transactivate a Hox gene directly (Subramanian *et al.,* 1995). In *Drosophila, cad* controls expression of homeobox-containing pair-rule genes such as *fushi tarazu,* which it regulates directly in embryos (Dearolf *et al.,* 1989) and the *vab-7* homolog *eve,* which it maintains during imaginal disc development (Moreno and Morata, 1999). During *Drosophila* gastrulation and hindgut formation, aspects of which may be homologous to *C. elegans* ventral cleft closure and rectal formation from the MS and ABp descendants, *caudal* regulates, possibly directly, transcription of the downstream patterning genes *fork head, wingless,* and *folded gastrulation* (Wu and Lengyel, 1998). It will be of interest to determine whether similar regulatory interactions are involved in *C. elegans* posterior morphogenesis.

REFERENCES

Ahnn, J., and Fire, A. (1994). A screen for genetic loci required for body-wall muscle development during embryogenesis in *Caenorhabditis elegans. Genetics* **137,** 483–498.

Ahringer, J. (1996). Posterior patterning by the *Caenorhabditis elegans even-skipped* homolog *vab-7. Genes Dev.* **10,** 1120–1130.

Ahringer, J. (1997). Maternal control of a zygotic patterning gene in *Caenorhabditis elegans. Development* **124,** 3865–3869.

Austin, J., and Kenyon, C. (1994). Cell contact regulates neuroblast formation in the *Caenorhabditis elegans* lateral epidermis. *Development* **120,** 313–323.

C. elegans Sequencing Consortium (1998). Genome sequence of the nematode *C. elegans:* A platform for investigating biology. *Science* **282,** 2012–2018.

Clark, S., Chisholm, A., and Horvitz, H. (1993). Control of cell fates in the central body region of *C. elegans* by the homeobox gene *lin-39. Cell* **74,** 43–55.

Cowing, D., and Kenyon, C. (1992). Expression of the homeotic gene *mab-5* during *Caenorhabditis elegans* embryogenesis. *Development* **116,** 481–490.

Davidson, E. (1991). Spatial mechanisms of gene regulation in metazoan embryos. *Development* **113,** 1–26.

Davidson, E. (1994). Molecular biology of embryonic development: How far have we come in the last ten years? *BioEssays* **16,** 603–615.

Dearolf, C. R., Topol, J., and Parker, C. S. (1989). Transcriptional control of Drosophila *fushi tarazu* zebra stripe expression. *Genes Dev.* **3,** 384–398.

Edgar, L. G. (1995). Blastomere culture and analysis. *In* "*Caenorhabditis elegans:* Modern Biological Analysis of an Organism" (H. F. Epstein and D. C. Shakes, Eds.), pp. 303–322. Academic Press, New York.

Evans, T., Crittenden, S., Kodoyianni, V., and Kimble, J. (1994). Translational control of maternal *glp-1* mRNA establishes an asymmetry in the *C. elegans* embryo. *Cell* **77,** 183–194.

Ferreira, H. B., Zhang, Y., Zhao, C., and Emmons, S. W. (1999). Patterning of *Caenorhabditis elegans* posterior structures by the *abdominal-B* homolog, *egl-5. Dev. Biol.* **207,** 215–228.

Fire, A. (1994). A 4-dimensional digital image archiving system for cell lineage tracing and retrospective embryology. *Comput. Appl. Biosci.* **10,** 443–447.

Fire, A., Harrison, S. W., and Dixon, D. (1990). A modular set of lacZ fusion vectors for studying gene expression in *Caenorhabditis elegans. Gene* **93,** 189–198.

Francis, G. R., and Waterston, R. H. (1985). Muscle organization in *C. elegans:* Localization of proteins implicated in thin filament attachment and I-band organization. *J. Cell Biol.* **101,** 1532–1549.

Gendreau, S., Moskowitz, I., Terns, R., and Rothman, J. (1994). The potential to differentiate epidermis is unequally distributed in the AB lineage during early embryonic development in *C. elegans. Dev. Biol.* **166,** 770–781.

Herman, R. (1987). Mosaic analysis of two genes that affect nervous system structure in *Caenorhabditis elegans. Genetics* **116,** 377–388.

Hope, I. A. (1991). 'Promoter trapping' in Caenorhabditis elegans. *Development* **113,** 399–408.

Hunter, C., and Kenyon, C. (1996). Spatial and temporal controls target *pal-1* blastomere-specification activity to a single blastomere lineage in *C. elegans* embryos. *Cell* **87,** 217–226.

Hunter, C. P., Harris, J. M., Maloof, J. N., and Kenyon, C. (1999). Hox gene expression in a single *Caenorhabditis elegans* cell is regulated by a *caudal* homolog and intercellular signals that inhibit Wnt signaling. *Development* **126,** 805–814.

Kenyon, C. (1986). A gene involved in the development of the posterior body region of *C. elegans. Cell* **46,** 477–487.

Kenyon, C., and Wang, B. (1991). A cluster of *Antennapedia*-class homeobox genes in a nonsegmented animal. *Science* **253,** 516–517.

Labouesse, M., Hartwieg, E., and Horvitz, H. R. (1996). The *Caenorhabditis elegans* LIN-26 protein is required to specify and/or maintain all non-neuronal ectodermal cell fates. *Development* **122,** 2579–2588.

Lehmann, R., and Gavis, E. (1994). Translational regulation of *nanos* by RNA localization. *Nature* **369,** 315–318.

Macdonald, P., and Struhl, G. (1986). A molecular gradient in early Drosophila embryos and its role in specifying the body pattern. *Nature* **324,** 537–545.

Manak, J., and Scott, M. (1994). A class act: Conservation of homeodomain protein functions. *Development* **Suppl.,** 61–71.

Masquera, L., Forristall, C., Zhou, Y., and King, M. (1993). A mRNA localized to the vegetal cortex of Xenopus oocytes encodes a protein with a nanos-like zinc finger domain. *Development* **117,** 377–386.

McGinnis, W., and Krumlauf, R. (1992). Homeobox genes and axial patterning. *Cell* **68,** 283–302.

Mello, C., and Fire, A. (1995). DNA transformation. *In* "*Caenorhabditis elegans:* Modern Biological Analysis of an Organism" (H. Epstein and D. Shakes, Eds.), Vol. 48d, pp. 451–482. Academic Press, New York.

Mlodzik, M., and Gehring, W. (1987). Expression of the *caudal* gene in the germ line of Drosophila: Formation of an RNA and protein gradient during early embryogenesis. *Cell* **48,** 465–478.

Moreno, E., and Morata, G. (1999). *Caudal* is the Hox gene that specifies the most posterior *Drosophila* segment. *Nature* **400,** 873–877.

Okkema, P., and Fire, A. (1994). The *Caenorhabditis elegans* NK-2 class homeoprotein CEH-22 is involved in combinatorial activation of gene expression in pharyngeal muscle. *Development* **120,** 2175–2186.

Perry, M., Li, W., Trent, C., Robertson, B., Fire, A., Hageman, J., and Wood, W. (1993). Molecular characterization of the *her-1* gene suggests a direct role in cell signaling during *Caenorhabditis elegans* sex determination. *Genes Dev.* **7,** 216–228.

Podbilewicz, B., and White, J. G. (1994). Cell fusions in the developing epithelia of *C. elegans. Dev. Biol.* **161,** 408–424.

Rose, L. S., and Kemphues, K. J. (1998). Early patterning of the *C. elegans* embryo. *Annu. Rev. Genet.* **32,** 521–545.

Salser, S., and Kenyon, C. (1996). A *C. elegans* Hox gene switches on, off, on and off again to regulate proliferation, differentiation and morphogenesis. *Development* **122,** 1651–1661.

Schauer, I., and Wood, W. (1990). Early *C. elegans* embryos are transcriptionally active. *Development* **110,** 1303–1317.

Schnabel, R., and Priess, J. R. (1997). Specification of cell fates in the early embryo. *In* "*C. elegans* II" (D. L. Riddle, T. Blumenthal, B. J. Meyer, and J. R. Priess, Eds.), pp. 361–382. Cold Spring Harbor Laboratory Press, Cold Spring Harbor, NY.

Subramanian, V., Meyer, B., and Gruss, P. (1995). Disruption of the murine homeobox gene Cdx1 affects axial skeletal identities by altering the mesodermal expression domains of Hox genes. *Cell* **83,** 641–653.

Sulston, J., and Hodgkin, J. (1988). Methods. *In* "The Nematode *Caenorhabditis elegans*" (W. B. Wood, Ed.), pp. 81–122. Cold Spring Harbor Laboratory Press, Cold Spring Harbor, NY.

Sulston, J., and Horvitz, H. (1977). Post-embryonic cell lineage of the nematode *Caenorhabditis elegans. Dev. Biol.* **56,** 110–156.

Sulston, J., Schierenberg, E., White, J., and Thomson, J. (1983). The embryonic cell lineage of the nematode *Caenorhabditis elegans. Dev. Biol.* **100,** 64–119.

Thomas, C., DeVries, P., Hardin, J., and White, J. (1996). Four-dimensional imaging: Computer visualization of 3D movements in living specimens. *Science* **273,** 603–607.

Van Auken, K., Weaver, D. C., Edgar, L. G., and Wood, W. B. (2000). *C. elegans* embryonic axial patterning requires two recently discovered posterior-group Hox genes. *Proc. Natl. Acad. Sci. USA* **97,** 4499–4503.

Wang, B., Muller-Immergluck, M., Austin, J., Robinson, N., Chisholm, A., and Kenyon, C. (1993). A homeotic gene cluster patterns the anteroposterior body axis of *C. elegans. Cell* **74,** 29–42.

Waring, D., and Kenyon, C. (1990). Selective silencing of cell communication influences anteroposterior pattern formation in *C. elegans. Cell* **60,** 123–131.

Waring, D., and Kenyon, C. (1991). Regulation of cellular responsiveness to inductive signals in the developing *C. elegans* nervous system. *Nature* **350,** 712–715.

Williams-Masson, E. M., Malik, A. N., and Hardin, J. (1997). An actin-mediated two-step mechanism is required for ventral enclosure of the *C. elegans* hypodermis. *Development* **124,** 2889–2901.

Wood, W. B. (1998). Handed asymmetry in nematodes. *Semin. Cell Dev. Biol.* **9,** 53–60.

Wu, L. H., and Lengyel, J. A. (1998). Role of *caudal* in hindgut specification and gastrulation suggests homology between Drosophila amnioproctodeal invagination and vertebrate blastopore. *Development* **125,** 2433–2442.

Yandell, M., Edgar, L., and Wood, W. (1994). Trimethylpsoralen induces small deletion mutations in *Caenorhabditis elegans. Proc. Natl. Acad. Sci. USA* **91,** 1381–1385.

Zhang, H., and Emmons, S. W. (2000). A *C. elegans* mediator protein confers regulatory selectivity of lineage-specific expression of a transcription factor gene. *Genes Dev.* **14,** 2161–2172.